EXPERIMENTAL DATA ON THE REFRACTION OF UNDERWATER EXPLOSION PULSES

by

R.M. Barash and J.A. Goertner
Naval Ordnance Laboratory
White Oak, Silver Spring, Maryland, U.S.

There are several reasons why a researcher in underwater acoustics might be interested in the use of explosion pulses as sources. The most generally recognized reason is that explosions are convenient and powerful sources of broad-spectrum sound energy. Usually, however, the received signals are filtered for analysis — for example, through one-octave or one-third octave band filters — to correspond to the characteristics of a sonar application of interest.

By contrast, the Underwater Explosions Division of the Naval Ordnance Laboratory, as well as some other groups, has direct interest in the propagation of underwater explosion pulses as such. For our purposes, we make broadband recording of the received pulses. Generally, the lower limit of the recorded frequency spectrum is practically zero; the upper limit varies from about 20 kHz, in the case of an FM recording on magnetic tape, to more the 100 kHz, for a film record of an oscilloscope trace.

With recordings of this type there are additional reasons why explosion pulses are useful sources for propagation experiments. There are kinds of information that usually show up clearly in our pulse records, but which might not be so easily or clearly obtainable, or perhaps not be obtainable at all, from sinusoidal sources or from narrow-band recordings of pressure pulses. The types of information we refer to are amplitudes, arrival times, arrival angles, and phase shifts, particularly if the received signal consists of two or more arrivals which overlap in time. Broadband explosion pulse recordings can give

enlightening answers to crucial questions concerning the validity of ray theory.

We will present some significant examples of results from U.S. experiments on the refraction of underwater explosion shock waves. In particular, we will show data that may be useful in evaluating the criteria for the conditions under which ray theory is considered valid. We shall confine our presentation mainly to a description of the data. An accompanying paper by Mr Blatstein, also of NOL, will describe a theoretical treatment of pulses under conditions for which ray tracing is not valid [see Session 4 of these Proceedings].

We will begin by describing an underwater explosion pressure pulse under non-refractive conditions; that is, in water of uniform sound velocity and of indefinite extent [Ref. 1]. Figure 1 shows a typical recording of pressure vs time measured at some distance from an underwater explosion. At the instant the shock wave pressure has subsided, there are additional smaller pulses emitted from the oscillating gas bubble that was formed by the explosion, but we shall not be concerned with these later pulses here. The exponentially-decaying shock wave pulse is described by the first equation in Fig. 1,

$$p(t) = p_m e^{-t/\theta}$$

where: $p(t)$ = the pressure above hydrostatic

p_m = the peak pressure above hydrostatic

θ = the exponential decay constant; i.e., the time at which the pressure has fallen to $1/e$ of the peak pressure.

The values of the parameters p_m and θ depend on the explosive composition, on the size of the explosive charge, and on the distance at which the pulse is observed. From many experiments, and by use of appropriate scaling laws, researchers have determined that the values of p_m and θ are given by the simple formulae shown here. W is the weight of the explosive charge, and R is the radial distance from the charge to the point of observation. The quantity $(W^{1/3}/R)$ is required by scaling considerations. K_p and K_θ are constants which depend on the charge composition.

In the expression for p_m, the exponent 1.13 requires an explanation. If, instead, we had an exponent of only 1, then the expression would represent a case in which there were no losses, but only geometrical spreading. The pressure would be equal to $K_p^{1/3}$, which is a reference pressure at unit distance, divided by R, which accounts for spherical spreading. But in the case of an explosion pulse there are significant losses. As the shock wave propagates, a substantial amount of energy is dissipated at the shock front. At larger distances, when the pressure has become small enough that the pulse can be considered an acoustic rather than a finite amplitude pulse, there are absorptive losses — the same type of frequency-dependent attentuation that is familiar in acoustics. It turns out that the combined losses of both types can be adequately described over a rather wide range of distances by using this equation with an exponent of 1.13. In the equation for the time constant, θ, the small negative exponent indicates that the decay time increases slightly as the pulse propagates. This occurs because each portion of the pulse propagates at a slightly different velocity depending on its own finite value of pressure.

This, then, is an explosion pulse in isovelocity water of infinite extent. What about a pulse reflected at the water surface? This is illustrated at the left in Fig. 2. The top pulse is a direct pulse. Just below it is a pulse arriving at the same point, but along a surface-reflected path. This pulse is inverted because its phase has been shifted by π radians. Its arrival time is later, and its amplitude is smaller, because of the longer travel path. At the receiver the two arrivals are superimposed to give the resultant pulse shown at the bottom. The reflected pulse may be large enough to reduce the resulting pressure to a negative value, as indicated by the dashed curve. But water cannot sustain this tension, and so it cavitates. Hence, we observe only the solid-line pulse, which usually goes no lower than about zero absolute pressure.

On the right side of this figure is an example of a bottom-reflected explosion pulse. Various degrees of phase shift are possible. When a non-sinusoidal pulse is shifted by a phase angle which is independent of frequency, the pulse form is necessarily distorted [Ref. 2].

With this background, let us consider refraction effects. The two pioneering U.S. experiments on the refraction of underwater explosion pulses were done with small scale simulations of oceanic conditions. The University of New Hampshire used a laboratory tank and set up an artificial thermal gradient. The Woods Hole Oceanographic Institution used a flooded quarry having a summer thermal structure very similar to that of the upper few hundred metres of the ocean. We will show data from the Woods Hole quarry experiment [Ref. 3]. Figure 3 shows a representative sound velocity profile and ray diagram from this experiment. TNT charges were placed at a few different depths and pressure gauges were placed at many positions throughout this ray pattern. In the upper half of Fig. 4 we see the most interesting portion of the ray diagram. The dots indicate gauge positions; corresponding pulse recordings are shown in the lower part of the figure.

This was an exploratory experiment that revealed marked differences in the charcter of pressure pulses observed in different regions of the pressure field. Look first at the closest two ranges, the first two columns of pulses. The undistorted character of these pulses is consistent with the corresponding portion of the ray diagram above. There is slight bending of the rays in this region but nothing severe. However, if we look at the right half of the ray diagram, we can see three features of interest: first, a region of highly divergent rays, perhaps a shadow region; second, just below it, a caustic region; and third, just below that, a region of intersecting ray groups.

Let us look at the pressure pulses recorded at these positions, starting with the highest amplitude pulse about half way down the fourth column. This was evidently recorded at a caustic. Above the caustic pulse are pulses in which the initial abrupt rise in pressure is very small. This is followed by a slow rise in pressure, to a value that is generally not so great as in isovelocity water. These pulses have the appearance of having had the high frequency energy removed while the low frequency energy is retained. These are shadow zone pulses. Now, looking at the pulses below the caustic pulse, we see that these appear to have two peaks. This is consistent with the corresponding portion of the ray diagram which shows two intersecting groups of rays. In this region we would expect to receive, at any

given point, more than one signal, each one travelling over a different path and arriving at a generally different time.

Figure 4b repeats on a larger scale the lower portion of the previous figure. The solid-line pulses are the recorded ones; the dashed lines indicate the pulses that would have been recorded at these same positions if the water had had uniform sound velocity. Thus, the effect of refraction is shown by the difference between each recorded solid-line pulse and its reference isovelocity pulse.

Looking again at the first two columns of pulses, those associated with the region containing slightly bent rays, we see that the pulses are relatively undistorted, with amplitudes only slightly affected by refraction. The cutoff in the top pulse of the first column, the top two pulses in the second column, and so on, are due simply to surface-reflected arrivals.

Now let us look again at the pulses recorded in the right half of the ray diagram. Note the high amplitude caustic pulse about half way down the fourth column. The peak pressures recorded at caustics throughout this experiment were up to four times as great as would have been expected at the same points in isovelocity water. Above the caustic pulse we see the shadow zone pulses and how they compare with the corresponding unrefracted pulses. Below the caustic we see the effect of multiple arrivals on the shape of the pressure pulse.

The characteristics of pressure pulses at caustics, and in the regions just above and below, is of sufficient interest that the Naval Ordnance Laboratory later performed a similar experiment, also in a quarry, but with a large number of very finely spaced gauges placed at the caustic on each shot [Ref.4].

Figure 5 shows a ray diagram for the NOL quarry experiment. The velocity profile was very similar to the Woods Hole profile, but it was smoother, and therefore, the ray diagram showed a smoother and better defined caustic. A vertical array of gauges, with a spacing interval of only inches, was placed at positions such as illustrated in Fig. 5. A typical set of pulse recordings is shown at the right.

Although these pulses are not positioned according to actual relative arrival times, this information is available from the original recordings. The upper pulses were recorded in the caustic regions. We found that peak pressure amplification due to refraction varied from 3.5 for the larger charges — 50 lbs — to about 6 for the smallest charges we used — 1/8 lb. The pulses shown here, from an 8-lb charge, exhibit a pressure amplification of about 5.

The pulses recorded just below the caustic region exhibit two arrivals. Because the time of each arrival is so clearly defined on each record, the calculated and observed arrival times can be clearly compared, and the angle of arrival of each of the two wave fronts can be determined. As for amplitudes, the jump in pressure from each of the two arrivals can be measured separately and compared with theoretical predictions.

How does the peak pressure, that is, the maximum pressure in the pulse, vary with gauge depth around the caustic? Figure 6 summarizes the data for all the 1/8-lb shots fired at a source depth of 35 feet and measured at a horizontal distance of 190 ft from the explosion. These three curves are plotted as a function of gauge depth relative to the depth at which the highest pressure was observed. The middle curve shows the pressure factor, the factor by which refraction has increased the peak pressure in the pulse relative to the value for isovelocity water. The maximum is 6; it falls off to half that amount about one foot into the double-arrival region, plotted toward the right, more rapidly in the shadow zone, plotted toward the left. Conventional ray tracing, used without correction, predicts infinite pressure at the caustic. Data such as presented here can be quite useful in evaluating the limitations of ray theory and the validity of other approaches.

In regions of moderate refractive convergence and divergence, the pressure at the peak of the exponential pulse is predicted well by the use of ray tracing, taken together with a straightforward modification to account for the 1.13 exponent in the equation for peak pressure vs distance. The conventional ray-tracing prediction of infinite amplitude at the caustic does not occur in reality, and we have instead the finite pressure amplification indicated by the rounded peak on this middle curve. In the shadow zone, represented by the left slope of this curve, conventional ray tracing predicts

zero pressure. The actual pressures observed in this region are those contributed by the low frequency components of the pulse, as is evident from the pulse shapes; this is also consistent with the consideration that conventional ray tracing is a high frequency approximation. A method for use in the caustic and shadow regions is described in Mr. Blatstein's paper.

The top curve in Fig. 6 shows the energy factor. This is the factor by which the energy flux density in the pulse has been increased by refraction, relative to its magnitude in isovelocity water. Here the maximum is 9. The lowest curve, which represents the impulse factor, is quite interesting. By impulse we mean the impulse per unit area carried by the pulse across the gauge point. It is measured as the integral of pressure with respect to time in the pulse, or the area under the pressure vs time curve. There is no noticeable peak in impulse with variation of gauge location through the caustic. Refraction appears to have no significant effect on impulse. It is observed that at a caustic, where peak pressure is increased because of refraction, the decay constant decreases in a compensating manner, so that the impulse remains unaffected.

The final experiment we will describe is an ocean experiment, also by the Naval Ordnance Laboratory [Ref. 5]. Figure 7 shows the sound velocity profile and the pertinent rays from the ray diagram. One pound, eight pound and 900 pound charges were fired in the Sargasso Sea at depths including 1000 feet. At the convergence zone 33 n.mi away, pressure pulses were recorded from a 200-ft long vertical array of 100 hydrophones which spanned the depth of the caustic.

Figure 8 shows a series of pulse records from one 900-lb shot. Although all time scales are the same, the records are not positioned to show time relationships among different gauge locations. Such information is obtainable, however, from the original recordings. Each record shown here consists of both a direct and a reflected pulse, the second being inverted because of phase shift upon reflection at the water surface. Reflected pulses are, of course, also subject to refractive effects. The symmetry of direct and reflected signals in each of the upper records is due to the fact that the hydrophone string was suspended, by intention and good fortune, from the point at which the caustic intersected the surface. Thus, on this particular shot, it

turned out that the direct pulses are in the double-arrival region associated with the direct caustic, and the reflected pulses are in the shadow region associated with the reflected caustic. The top record was obtained 2 ft below the surface, just at about the caustic point; here there is almost complete mutual cancellation. As we look down the string of records, we see that the direct pulse and the reflected pulse become more and more separated in time. We also see that the double arrivals on the direct pulse become more distinct and that the time difference between them also increases. As for the inverted shadow-zone pulse, it becomes weaker and less sharp.

In the oceanic convergence zone experiment, the highest pressure amplification that we observed at the caustic was about 12.

The pulse shapes contain much information, and some useful inferences can be made from them. For example, Fig. 9 shows several pulses from NOL's quarry and convergence zone experiments [Ref. 6]. The solid lines represent the observed pulses, all recorded in double-arrival regions adjacent to caustics. The dashed curves are calculated pulses, constructed to test a theory regarding phase shift. The hypothesis was that the first arrival is undistorted, while the second undergoes a phase shift of $\pi/2$ as it passes through the caustic. From this comparison of pulse shapes, it was concluded that the data are consistent with the hypothesis. It would not have been possible to perform such an analysis if the source had been a continuous sinusoidal signal. In the case of a sinusoidal wave, two arrivals with different amplitudes, different travel times, and different phases, would blend into a single sinusoidal signal at the receiver. No type of processing can extract from such a record information on the amplitude and phase of each of the contributing signals. With an explosion pulse, however, various anlytical techniques can be devised, and this was an example of one.

As a final example of the usefulness of explosive sources in studying acoustic refraction, we will present some frequency spectra of recorded explosion pulses. Figure 10 shows three pulses recorded from a 900-lb shot during NOL's oceanic convergence experiment [Ref. 5].

To the right of each pulse is the corresponding energy spectrum calculated digitally from the broadband pulse record. The pulses are arranged here in order of increasing depth. The top one is from the shadow zone, the middle one from the caustic region, and the bottom one was recorded in the double-arrival region. Remember that we are not including bubble pulses, which would contribute much more low frequency energy than shown here.

Let us look first at the middle record, the pulse from the caustic region. It is basically an exponentially decaying pulse. The energy spectral density, as expected, decreases as frequency increases.

Now let us consider the pulse at the top, the shadow zone pulse. At low frequency, the energy density is as great as it is for the caustic pulse, but much of the higher frequency energy is missing. Incidentally, the lobe at 4 to 5 kHz is simply attributable to the spurious ringing seen on the record, which was due to resonance in the hydrophone mounting.

Finally, let us consider the pulse at the bottom, which contains two arrivals. The presence of these two steep features on the pulse, separated by a time interval of almost one ms, gives rise to a periodic pattern in the energy spectrum. The spectrum exhibits deep notches at integral multiples of the reciprocal of this time interval.

This has important implications. We recall that as the point of observation moves from the caustic through the double-arrival region, the time difference between the two arrivals increases. The energy spectra of these pulses will exhibit corresponding changes in the spacing and positions of the notches and peaks. Thus, if one is interested in reception in some particular narrow frequency band, a slight shift in receiver position might shift the periodic pattern in the spectrum by enough to make a 10 dB to 20 dB change in the received energy.

If the source were a continuous sinusoidal signal, this variation in received energy could simply be described as constructive and destructive interference. The received signal would be a sinusoidal

wave, from which the characteristics of the two interfering waves could not be extracted. But by using an explosive source, and by analysing digitally as we have shown here, we determine the received energy as a function of frequency over a broad spectrum, but we can also gain an understanding of how the pattern of the spectral curve is related to particular features which are directly observable in the recorded pulse.

We have described some of the experimental data on refraction of underwater explosion pulses. We have shown pressure pulses recorded at shadow zones, caustics, single-arrival and double-arrival regions. In particular, we have shown how the recorded pulses provide information on pressure amplification, arrival time, arrival angle, and phase shift, for each arrival in a double-arrival pulse. And we have indicated how data of this type can be especially useful in understanding the refractive propagation of underwater acoustic waves.

REFERENCES

1. R.H. Cole, "Underwater Explosions", Princeton University Press, N.J., 1948; also published by Dover Publications, Inc., New York, 1965.

2. A.B. Arons and D.R. Yennie, "Phase Distortion of Acoustic Pulses Obliquely Reflected from a Medium of Higher Sound Velocity", J.Acoust.Soc.Am., Vol. 22, 1955, pp. 231-237.

3. R.R. Brockhurst, J. Bruce, and A.B. Arons, "Refraction of Underwater Explosion Shock Waves by a Strong Velocity Gradient", J.Acoust.Soc.Am., Vol. 33, 1961, pp. 452-456.

4. R.M. Barash, and J.A. Goertner, "Refraction of Underwater Explosion Shock Waves: Pressure Histories Measured at Caustics in a Flooded Quarry", Naval Ordnance Laboratory Technical Report 67-9. April 1967.

5. R. Thrun, "Refraction of Underwater Explosion Shock Waves: Sargasso Sea Measurements", Naval Ordnance Laboratory Technical Report 71-102.

6. R.M. Barash, "Evidence of Phase Shift at Caustics", J.Acoust.Soc.Am., Vol. 43, Feb. 1968, pp. 378-380 (L), and "Reply to 'Comments on Evidence of Phase Shift at Caustics'", J.Acoust.Soc.Am., Vol. 44, Aug. 1968, pp. 643-644 (L).

DISCUSSION

When asked to what range the $(\frac{W^{1/3}}{R})^{1.13}$ could be used in peak pressure calculations, the second author replied that measurements with relatively refraction-free vertical paths indicated that the expression was still valid at $\frac{W^{1/3}}{R} = 2.5 \times 10^{-5}$ lb$^{1/3}$ ft^{-1}, provided also that $R \leq 20\,000$ ft

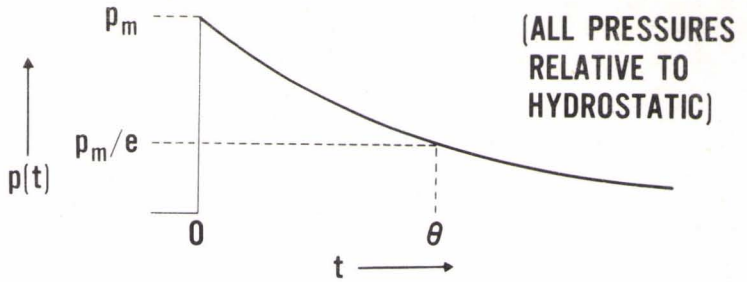

FIG. 1

$$p(t) = p_m e^{-t/\theta}$$

$$\text{WHERE} \quad p_m = K_p \left(\frac{W^{1/3}}{R}\right)^{1.13}$$

$$\text{AND} \quad \theta = K_\theta W^{1/3} \left(\frac{W^{1/3}}{R}\right)^{-0.22}$$

EXPLOSION PULSE IN ISOVELOCITY WATER

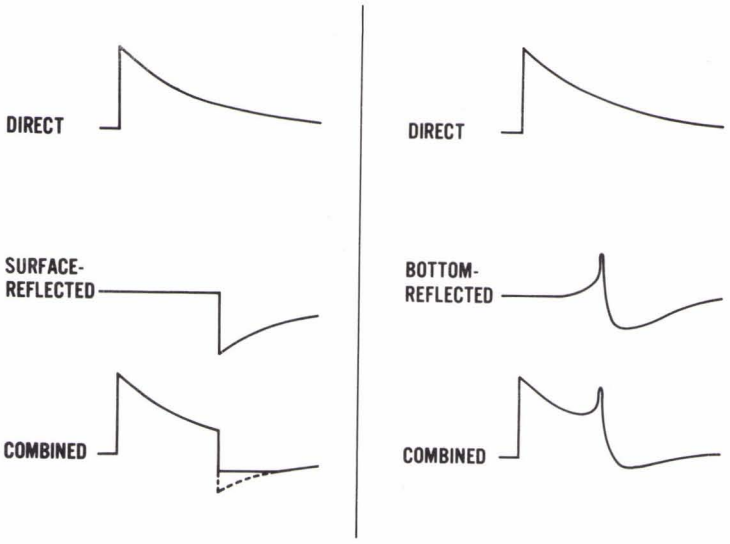

FIG. 2

REFLECTED PULSES

WHOI QUARRY EXPERIMENT

FIG. 3

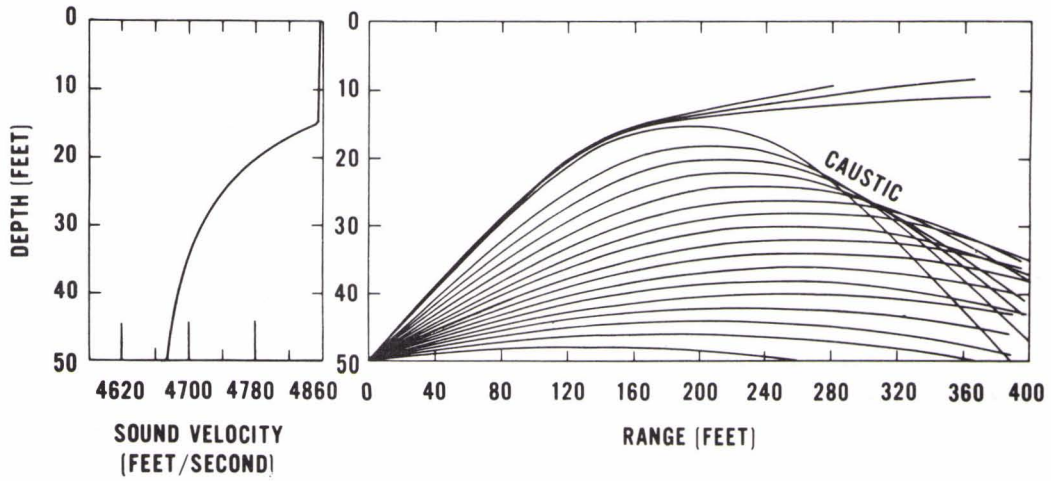

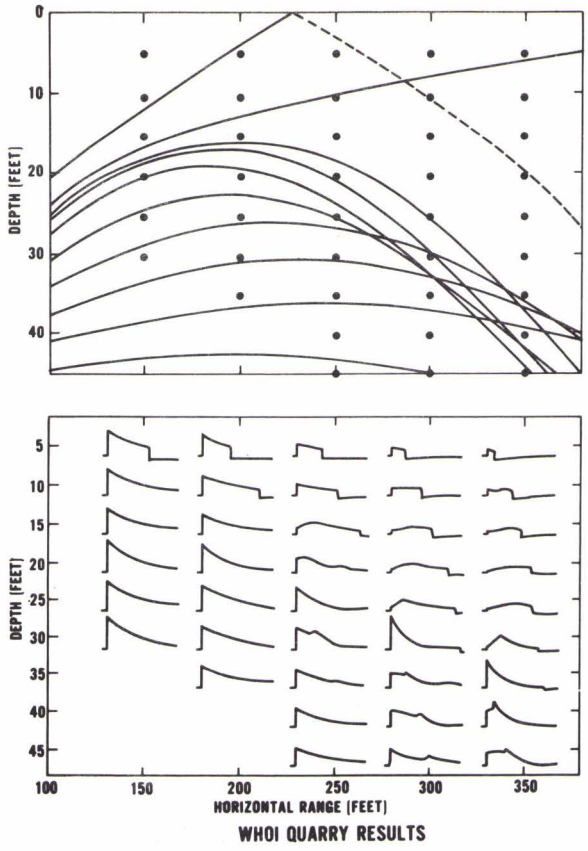
DEPTH (FEET)
0
10
20
30
40
DEPTH (FEET)
5
10
15
20
25
30
35
40
45
100
150
200
250
300
350
HORIZONTAL RANGE (FEET)
WHOI QUARRY RESULTS

FIG. 4

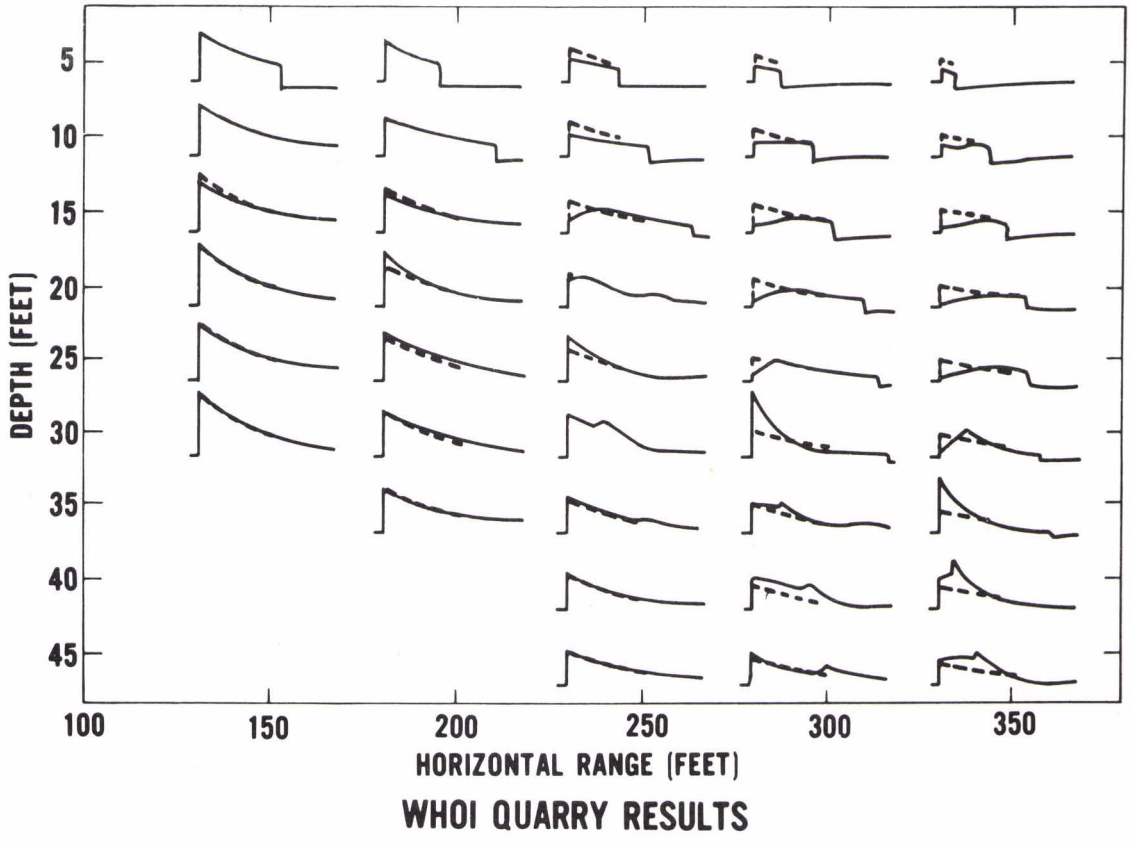
DEPTH (FEET)
5
10
15
20
25
30
35
40
45
100
150
200
250
300
350
HORIZONTAL RANGE (FEET)
WHOI QUARRY RESULTS

FIG. 4(b)

FIG. 5

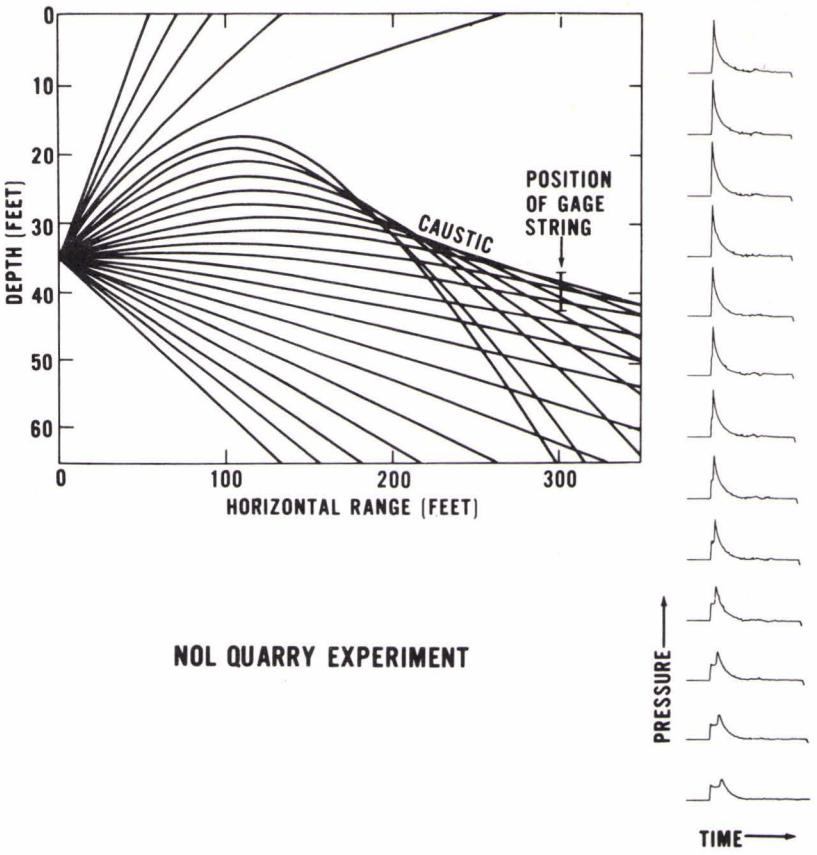

NOL QUARRY EXPERIMENT

NOL QUARRY RESULTS

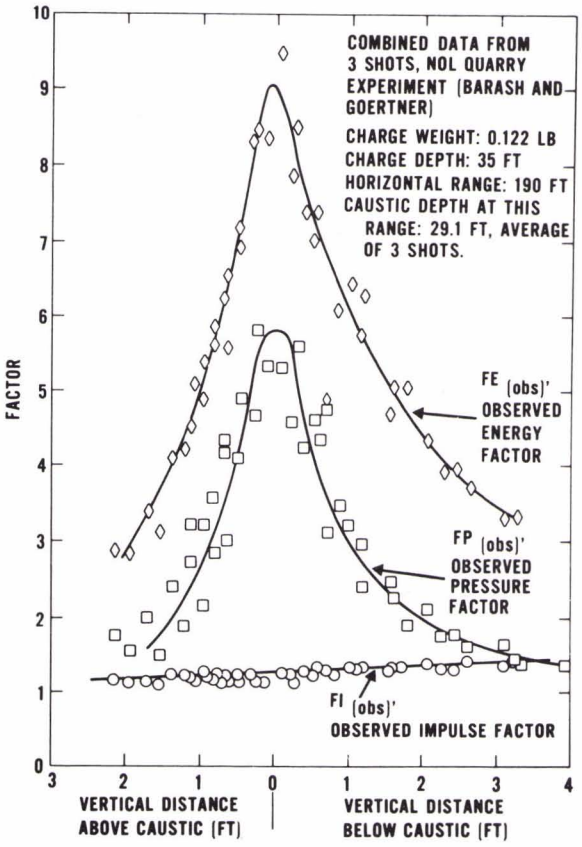

FIG. 6

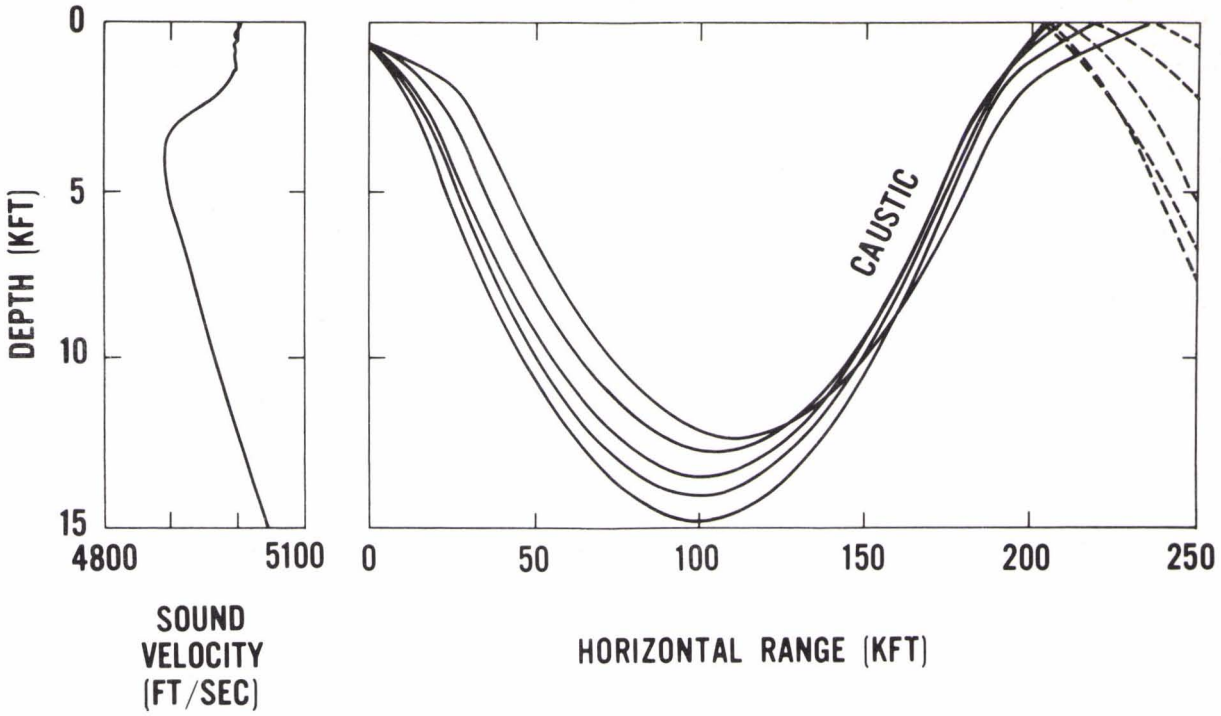

NOL CONVERGENCE ZONE EXPERIMENT

FIG. 7

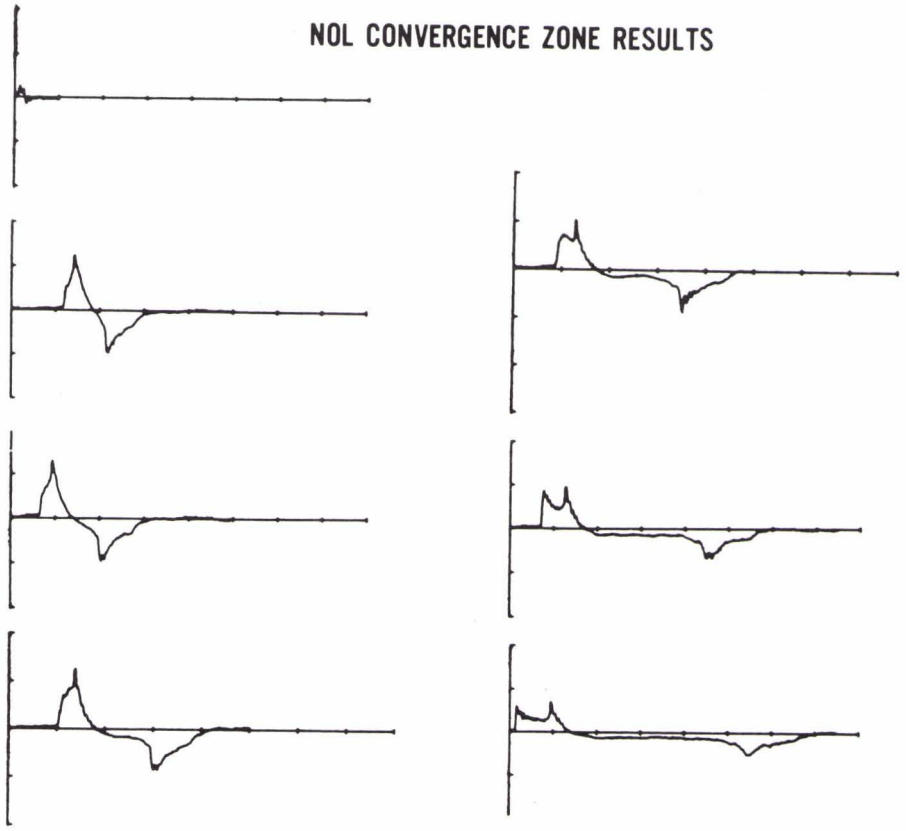

FIG. 8

RECORDED PULSES COMPARED WITH PHASE SHIFT CALCULATIONS

FIG. 9

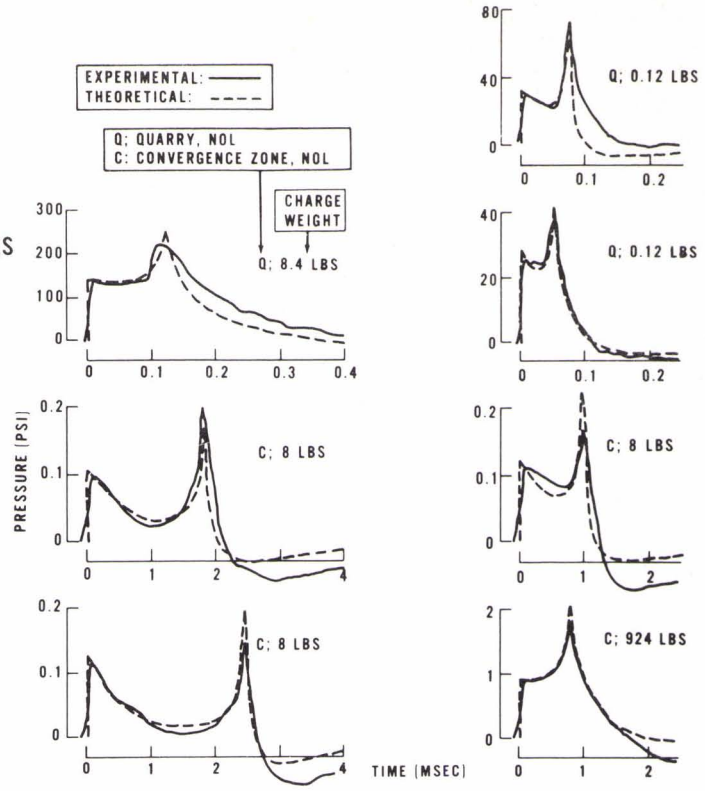

ENERGY SPECTRA OF REFRACTED PULSES

FIG. 10